1 **Formation of Organic Sulfur Compounds through SO₂ Initiated**

2 **Photochemistry of PAHs and DMSO at the Air-Water Interface**

5 Haoyu Jiang[1,2,3], Yingyao He[4], Yiqun Wang[1,2], Sheng Li[5], Bin Jiang[1,2], Luca Carena[6], Xue

6 Li[7], Lihua Yang[4], Tiangang Luan[4], Davide Vione[6], Sasho Gligorovski[*,1,2,3]

8 [1]State Key Laboratory of Organic Geochemistry and Guangdong Provincial Key Laboratory of

9 Environmental Protection and Resources Utilization, Guangzhou Institute of Geochemistry,

10 Chinese Academy of Sciences, Guangzhou 510 640, China

11 [2]Guangdong-Hong Kong-Macao Joint Laboratory for Environmental Pollution and Control,

12 Guangzhou Institute of Geochemistry, Chinese Academy of Science, Guangzhou 510640,

13 China

14 [3]Chinese Academy of Science, Center for Excellence in Deep Earth Science, Guangzhou,

15 510640

16 [4]School of Marine Sciences, Sun Yat-sen University, Guangzhou 510006, China

17 [5]Hunan Research Academy of Environmental sciences, Changsha, 410004, China

18 [6]Dipartimento di Chimica, Università di Torino, Via Pietro Giuria 5, 10125 Torino, Italy

19 [7]Institute of Mass Spectrometry and Atmospheric Environment, Jinan University, Guangzhou

20 510632, China

25 *Corresponding author:
26 Sasho Gligorovski
27 gligorovski@gig.ac.cn

29 **ABSTRACT**

30 The presence of organic sulfur compounds (OSs) at the water surface, acting as organic

31 surfactants, may influence the air-water interaction and contribute to new particle formation in

32 the atmosphere. However, the impact of ubiquitous anthropogenic pollutant emissions, such as

33 SO_2 and polycyclic aromatic hydrocarbons (PAHs) on the formation of OSs at the air-water

34 interface still remains unknown. Here, we observe large amounts of OSs formation in presence

35 of SO_2, upon irradiation of aqueous solutions containing typical PAHs such as pyrene (PYR),

36 fluoranthene (FLA), and phenanthrene (PHE), as well as dimethylsulfoxide (DMSO). We

37 observe rapid formation of several gaseous OSs from light-induced heterogeneous reactions of

38 SO_2 with either DMSO or a mixture of PAHs/DMSO, and some of these OSs (e.g.

39 methanesulfonic acid) are well established secondary organic aerosol (SOA) precursors. A

40 myriad of OSs and unsaturated compounds are produced and detected in the aqueous phase.

41 The tentative reaction pathways are supported by theoretical calculations of the reaction Gibbs

42 energies. Our findings provide new insights into potential sources and formation pathways of

43 OSs occurring at the water (sea, lake, river) surface, that should be considered in future model

44 studies to better represent the air-water interaction and SOA formation processes.

45

46 **Keywords:** PAHs, SO_2, SOA, aromatic organosulfates, water surface, photochemical reactions,

47 SPI-TOF-MS, FT-ICR-MS

48

1. INTRODUCTION

49

50 Organic sulfur compounds (OSs) are ubiquitous in atmospheric aerosols, and organosulfates

51 are considered as important tracers of secondary organic aerosols (SOA). Based on the

52 occurrence of hydrophilic and hydrophobic moieties in the same molecule, OSs are surface-

53 active compounds that cause reductions of surface tension and enhance the formation potential

54 of cloud condensation nuclei (CCN) in aerosol particles (Bruggemann et al., 2020).

55 Both biogenic and anthropogenic sources such as biomass and fossil fuel burning release OSs

56 into the atmosphere (Bruggemann et al., 2020). The contribution of aromatic organosulfates

57 could be up to two-thirds of the sum of the identified OSs (Riva et al., 2015; Riva et al., 2016),

58 and their input is highest during winter (Ma et al., 2014). Although some aromatic

59 organosulfates have similar chemical structures as those of potential aromatic VOC precursors,

60 such as toluene and xylene(Kundu et al., 2013), monocyclic aromatics were not regarded as

61 aromatic organosulfate precursors because they are more inclined to oxidize into ring-opening

62 products (Staudt et al., 2014; Kamens et al., 2011). Polycyclic aromatic hydrocarbons (PAHs),

63 such as naphthalene (NAP) and 2-methylnaphthalene (2-MeNAP) have rather been postulated

64 as the precursors of aromatic OSs (Riva et al., 2015; Staudt et al., 2014).

65 Among all aromatic compounds, PAHs are ubiquitous organics enriched at both the sea and

66 freshwater (lakes, river) surface (Cincinelli et al., 2001; Vácha et al., 2006; Chen et al., 2006;

67 Lohmann et al., 2009; Seidel et al., 2017), where they can reach even 200−400 times higher

68 concentrations compared to the water bulk (Cincinelli et al., 2001; Vácha et al., 2006; Chen et

69 al., 2006; Lohmann et al., 2009; Seidel et al., 2017; Hardy et al., 1990). The origin of PAHs

70 accumulated at the water surface stems from combustion processes such as biomass burning,

71 and coal- and petroleum-based combustion (Lammel, 2015). At the surface of freshwater and

72 seawater the PAHs concentrations vary, respectively, from 11.84 to 393.12 ng L^{-1} (Li et al.,

73 2017b), and from 5 to ~1900 ng L^{-1} (Valavanidis et al., 2008; Otto et al., 2015; González-Gaya

74   et al., 2019; Pérez-Carrera et al., 2007; Ma et al., 2013). Phenanthrene (PHE), fluoranthene

75   (FLA) and pyrene (PYR) are the most commonly detected PAHs in the coastal surface micro-

76   layer (SML) (Guitart et al., 2007; Stortini et al., 2009), and they accounted for 92 to 96% of the

77   total PAHs amount in the coastal surface waters of Nigeria (Benson et al., 2014).

78   Dimethylsulfoxide (DMSO) is an ubiquitous OS compound at the sea surface (Lee et al., 1999),

79   which derives from degradation of phytoplankton (Andreae, 1980), photodegradation of

80   dimethyl sulfide (DMS) (Barnes et al., 2006; Brimblecombe and Shooter, 1986), and microbial

81   oxidation of DMS(Zhang et al., 1991). Because of high Henry's Law coefficient ($\approx 10^7\,\text{M atm}^{-1}$)

82   and mass accommodation coefficient (0.10), gaseous DMSO can be deposited on the sea- and

83   fresh-water surface where one finds enhanced DMSO concentrations(Legrand et al., 2001;

84   Davidovits et al., 2006; González-Gaya et al., 2016). Highest levels of DMSO are detected in

85   the ocean (1.5 to 532 nmol L^{-1}) (Hatton et al., 1996; Lee and De Mora, 1996; Andreae, 1980;

86   Asher et al., 2017), followed by detected levels in rivers (<2.5–210 nmol L^{-1}) (Andreae, 1980),

87   lakes (up to 180 nmol L^{-1}) (Richards et al., 1994), rainwater (2-4 nmol L^{-1}) (Ridgeway et al.,

88   1992), and aerosols (69–125 pmol m^{-3}) (Harvey and Lang, 1986). One of the main degradation

89   pathways of DMSO is the reaction with hydroxyl radicals (OH) (Barnes et al., 2006), yielding

90   methanesulfinic and methanesulfonic acids (Librando et al., 2004). Because the concentrations

91   of DMSO are 1-2 orders of magnitude higher than those of DMS, the photochemical oxidation

92   of DMSO may be a relatively more important process than the photo-oxidation of DMS (Lee

93   et al., 1999).

94   Sulfur dioxide (SO_2) is directly emitted into the atmosphere by anthropogenic sources such as

95   fossil fuel combustion, coal, oil, and industrial processes (Smith et al., 2001). In addition, it can

96   also be formed during the oxidation of DMS (Hoffmann et al., 2016; Chen et al., 2018). As a

97   key contributor to aerosol nucleation, the role of SO_2 at the air-water interface is also recognized

98   as an efficient precursor of HOSO and OH radicals, following light absorption below 340 nm

99   and its excitation to a very reactive triplet state ($^3SO_2^*$) (Martins-Costa et al., 2018; Kroll et al.,

100   2018). A majority of studies employed sulfate-containing seed particles to explore the

101   formation pathway of OSs, while only a few were focused on the organosulfur formation

102   pathway that is unique to SO_2 chemistry (Blair et al., 2017; Shang et al., 2016; Passananti et al.,

103   2016). Some previous studies have found that the heterogeneous reaction of SO_2 with

104   unsaturated acids can lead to the formation of OSs in the atmosphere (Shang et al., 2016;

105   Passananti et al., 2016). However, it has also been found that monocyclic compounds such as

106   terephthalic acid are not reactive *via* direct SO_2 addition (Passananti et al., 2016), and there is

107   still a knowledge gap concerning other OSs formation pathways involving heterogeneous SO_2

108   oxidation. Indeed, air quality models cannot explain the quick increase of sulfate amount in

109   going from clean air to hazy events, when applying only the gas-phase and aqueous-phase

110   chemistry of SO_2 (Wang et al., 2014; Li et al., 2017a).

111   Several studies have assessed the heterogeneous chemistry of atmospherically relevant oxidants

112   with PAHs (Donaldson et al., 2009; Monge et al., 2010; Styler et al., 2011; Zhou et al., 2019).

113   Recently, Mekic et al (2020) and Jiang et al., (2021) have shown that the photosensitized

114   degradation of DMSO by excited triplet state of typical PAH compounds (fluorene ($^3FL^*$),

115   $^3PHE^*$, $^3FLA^*$ and $^3PYR^*$) leads to the formation of OSs compounds, among the others, in

116   both the gas- and aqueous- phase.

117   In this study we investigated the formation of OSs from aqueous DMSO and/or PAHs/DMSO,

118   initiated by gaseous SO_2 in the dark and in the presence of simulated sunlight irradiation

119   (300nm<λ<700nm). The gaseous OS products were assessed by membrane inlet single photon

120   ionization-time of flight-mass spectrometry (MI-SPI-TOFMS) (Zhang et al., 2019; Mekic et al.,

121   2020a; Jiang et al., 2021). The formed aqueous-phase products were evaluated by means of

122   ultrahigh resolution electrospray ionization Fourier-transform ion cyclotron resonance mass

123   spectrometry (FT-ICR-MS) (Jiang et al., 2016). The tentative reaction pathways of the formed

124 OSs during the heterogeneous SO_2 oxidation of PAHs/DMSO under actinic illumination are

125 supported by theoretical calculations of the reaction Gibbs energies. We show that oxidation by

126 SO_2 of PAHs/DMSO can release gaseous OSs, such as methanesulfonic acid (MSA), which are

127 known precursors of secondary organic aerosols (SOA) in the atmosphere. The formation of an

128 important number of OSs and unsaturated compounds, among the others, was observed in the

129 aqueous phase. We highlight the large amounts of generated linear and aromatic OSs, with

130 potential to greatly influence the air-water exchange of organic compounds.

131

2. EXPERIMENTAL

2.1. Photoreactor

A double-wall rectangular ($5 \times 5 \times 2$ cm) photoreactor was used to assess the reaction of gaseous

SO_2 with a water/organic film containing DMSO or DMSO/PAHs.(Mekic et al., 2020a; Mekic

et al., 2020b) The photoreactor was thermostated at ambient temperature (T = 293 K) by

thermostated bath (LAUDA ECO RE 630 GECO, Germany).

A SO_2 flow of 150 mL min^{-1} mixed with an air flow of 750 mL min^{-1} (0-1 L min^{-1} HORIBA

METRON mass flow controller; accuracy, $\pm 1\%$) allowed for dilution of SO_2 from a standard

gas cylinder with 5 ppm concentration to a mixing ratio of ~800 ppb that was flowing through

the photoreactor. The applied mixing ratio of 800 ppb is higher compared to the atmospheric

background mixing ratio that ranges from 1 to 70 ppb, but it is smaller than the SO_2 mixing

ratio in dilute volcanic plumes (for instance, a mixing ratio of ca. 10 ppm is observed about 10

km away from volcanic sources) (Oppenheimer et al., 1998), and it is also smaller compared to

some previous laboratory studies that used 7.7-500 ppm of SO_2 (Librando et al., 2014). The

applied mixing ratio of 800 ppb would probably amplify the intensity of the detected product

compounds, but the formation profiles would still remain the same as in the case of smaller SO_2

mixing ratios.

The concentration of PHE, FLA, and PYR (Sigma-Aldrich) used separately was 1×10^{-4} mol L^{-1}.

The three compounds were dissolved individually in a mixture of DMSO and ultrapure water

with proportion 10:90 v/v (Mekic et al., 2020b). Such high DMSO concentration was necessary

to dissolve the poorly water soluble PHE, FLA, and PYR (Mekic et al., 2020a; Mekic et al.,

2020b). Several previous studies also used high concentrations of the organic co-solvent to

assess the co-solvent effect on PAHs photolysis (Donaldson et al., 2009; Librando et al., 2014;

Grossman et al., 2016). The reactor was filled with 10 mL of freshly prepared DMSO/PAH

solution and irradiated with a Xenon lamp (Xe, 500 W, 300nm<λ<700nm) during the SO_2

157   oxidation of PAHs/DMSO. The spectral irradiance of the Xe lamp was measured with a

158   calibrated spectroradiometer (Ocean Optics, USA) equipped with a linear-array CCD detector,

159   and compared to the sunlight radiation (Mekic et al., 2020a; Mekic et al., 2020b). The

160   irradiation time of the aqueous solution was 2 hours.

161   Blank experiments of SO_2 reaction were carried out with aqueous DMSO in all experimental

162   conditions and with ultrapure water in the dark. All experiments were performed at least twice.

163   **2.2. Single Photon Ionization-Time of Flight-Mass Spectrometry (SPI-ToF-MS)**

164   A SPI-ToF-MS instrument (SPIMS 3000, Guangzhou Hexin Instrument Co., Ltd., China) was

165   used to detect the gas-phase compounds formed during the light-induced heterogeneous

166   reaction of SO_2 with PAHS/DMSO. The SPI-ToF-MS instrument was explained in details in

167   our previous studies (Deng et al., 2021; Mekic et al., 2020a), so here only brief description is

168   given in the supporting information (SI).

169   **2.3. Fourier‑Transform Ion Cyclotron Resonance Mass Spectrometry (FT-ICR-MS)**

170   As FT-ICR-MS was described in our previous paper, a brief description only is given in the SI.

171   An in-house software was used to calculate all mathematically possible formulae for all ions

172   with a signal-to-noise ratio above 10, using a mass tolerance of ± 0.2 ppm. Data of blank samples

173   were subtracted from those of all samples according to the same possible formulae.

174   The double bond equivalent (DBE) of a chemical formula $C_cH_hO_oN_nS_s$ is calculated using the

175   following equation (Yassine et al., 2014):

176    $DBE = \frac{2c+2-h+n}{2}$ (Eq-1)

177   The aromaticity equivalent (X_c) is calculated using the following equation:

178    $X_c = \frac{3[DBE-(mO+nS)]-2}{DBE-(mO+nS)}$ (Eq-2)

179   where X_c is introduced to improve the identification and characterization of aromatic and

180   condensed aromatic compounds, while *m* and *n* are the respective fractions of oxygen and sulfur

181   atoms that are involved in the π-bonds of a molecular structure (Yassine et al., 2014). According

182   to the model structural classes, the values of m and n were all set to 0. Threshold values of X_c

183   between 2.5 and 2.7 ($2.5 \leqslant X_c < 2.7$) and equal or greater than 2.7 ($X_c \geqslant 2.7$) were set as

184   minimum criteria for the presence of aromatics or condensed aromatic compounds in an

185   identified molecule (Blair et al., 2017; Jiang et al., 2016). It ought to be highlighted that electron

186   spray ionization (ESI) and desorption electrospray ionization (DESI) of OSs is especially

187   favorable in the negative-ion mode, making the observed fraction of OSs further amplified

188   (Blair et al., 2017).

189   **2.4. Theoretical Calculations**

190   The proposed structures of all identified tentative OSs are based on the reasonable inferred

191   elemental compositions for a single mass, following speculation through NIST Chemistry

192   WebBook (https://webbook.nist.gov/chemistry/mw-ser/) and database of MI-SPI-ToF-MS or

193   FT-ICR-MS. Considering that PHE, PYR, FLA and SO_2 can all absorb lamp radiation,

194   theoretical calculations were carried out to obtain some insights into the degradation pathways

195   of DMSO initiated by the excited triplet states $^3PHE^*$, $^3PYR^*$, $^3FLA^*$ and $^3SO_2^*$ in the aqueous-

196   and gaseous- phase, as well as the interaction between light-excited PAHs and SO_2.

197   All calculations shown here were assessed by Gaussian 16W package (Frisch et al., 2016). The

198   level of theory B3LYP/6-311G(d,p) was applied for geometry optimizations and frequency

199   calculations for all molecules depicted in the reaction scheme (Mclean and Chandler, 1980;

200   Binning Jr and Curtiss, 1990). There were no imaginary frequencies for all molecules optimized.

201   Single-point energy calculations were performed at a more expensive level, i.e., M06-2X/Def2-

202   TZVP level (Zhao and Truhlar, 2008; Weigend and Ahlrichs, 2005; Weigend, 2006). The

203   existence of possible geometric isomers and conformers for each species were considered and

204   investigated, and those with lowest calculated Gibbs free energies were selected. Molecular

205   oxygen (O_2), carbon dioxide (CO_2) and water molecules (H_2O) were placed as reactants or

206   products (if needed) to balance atoms in the schemes. Detailed Gibbs free energies for all

207   molecules are presented in Table S1 and S2, and the corresponding reaction Gibbs energies are

208   shown in Scheme 1.

209

3. RESULTS AND DISCUSSION

3.1. Gaseous OSs Detected by MI-SPI-ToF-MS

To detect the gas-phase compounds formed by heterogeneous SO_2 oxidation of PAHs/DMSO in the dark and under light irradiation, we applied MI-SPI-ToF-MS as a novel promising technology for the real-time monitoring of VOCs (Zhang et al., 2019; Mekic et al., 2020a; Deng et al., 2021).

Figure 1A shows the Venn diagrams of the observed number of m/z signals corresponding to the gas-phase products of the light-induced heterogeneous SO_2 oxidation of PAHs/DMSO. The Venn diagrams showing the comparison of the gaseous products formed under different conditions are presented in Figure S1. The biggest contributor to the total number of secondarily formed products is the light-induced SO_2 oxidation of DMSO (Figure 1B). Among all detected m/z signals (Table S4), we tentatively identified a number of unsaturated multifunctional molecules and OSs released in the gas phase from the reaction of SO_2 with either DMSO or PAHs/DMSO, which are summarized in Table S5. It should be noted, the possibility for the existence of isomers and of different molecular formulas for the compounds with the same molecular weight (Nizkorodov et al., 2011). We emphasize the formation of gaseous OSs, and especially of those that are known to be SOA precursors. For example, the m/z signals of 80, 94, 96, 112, 124, 126 were inferred as methanesulfinic acid (CH_3SO_2H, MSIA), methylsulfonylmethane ((CH_3)$_2SO_2$, MSM), methanesulfonic acid (CH_3SO_3H, MSA), hydroxymethanesulfonic acid (CH_4O_4S, MSAOH), ethyl methanesulfonate ($CH_3SO_3C_2H_5$, EMS) and 2-hydroxyethenesulfonic acid ($C_2H_5O_4SH$, ESAOH) (Berresheim et al., 1993; Berresheim and Eisele, 1998; Karl et al., 2007; Hopkins et al., 2008; Gaston et al., 2010; Ning et al., 2020; Dawson et al., 2012).
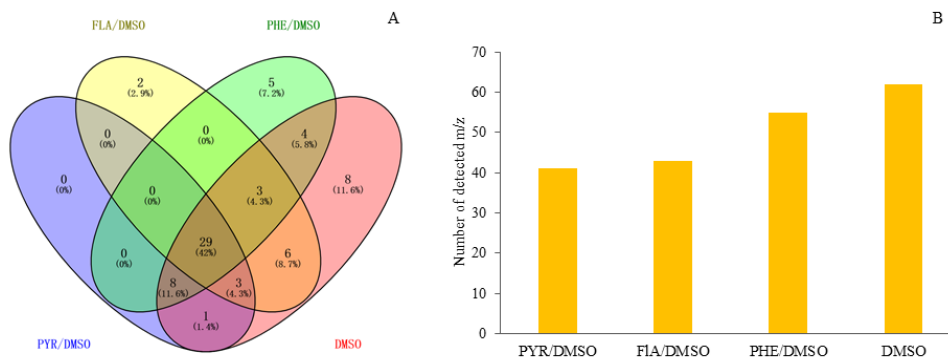
Figure 1: Venn Diagrams of the detected *m/z* signals in the gas-phase for the heterogeneous reaction of SO$_2$ with DMSO and PAHs/DMSO under light irradiation (300 nm<λ<700nm) (Panel A); The total number of identified *m/z* signals between the heterogeneous reactions of SO$_2$ with DMSO and PAHs/DMSO, under light irradiation (Panel B).

3.2. Formation Profiles of Gaseous OSs

In this study, we observed rapid formation of MSA, MSIA, MSM, EMS, MSAOH, and ESAOH (Figure 2 and Figure S2). The reaction of DMSO with OH leads to formation of MSIA (Barnes et al., 2006), which in turn may react again with OH radicals to form MSA (Librando et al., 2004; Barnes et al., 2006; Rosati et al., 2021). Gaseous MSA is a particularly important compound that can participate in the initial nucleation and growth step of particles, known as new particle formation (NPF) process (Schobesberger et al., 2013; Chen et al., 2016; Zhao et al., 2017; Perraud et al., 2015). Declining gaseous MSA concentrations were actually reported during marine NPF events, thereby suggesting that MSA may enter the aerosol particles at the earliest possible stage and significantly assist in cluster formation (Dall'osto et al., 2012; Bork et al., 2014). MSA is the simplest organosulfate compound, which can be mainly formed during the OH oxidation of DMS (Barnes et al., 2006; Rosati et al., 2021). Gas-phase MSA above the oceans and in coastal areas represents about 10 to 100% of the gas-phase sulfuric acid (SA)

252 concentration (Berresheim et al., 2002). It has been suggested that MSA can enhance particle

253 formation from SA by 15-300%, if equal quantities of SA and MSA are present (Bork et al.,

254 2014). There is a discrepancy between the modeled and measured concentration profiles of

255 MSA, which indicates a missing MSA source. This source seems to be much stronger than the

256 estimated production stemming from OH oxidation of DMS (Zhang et al., 2014a). Zhang et al.

257 (2014) suggested a strong daytime source of MSA, the precursor of which may be DMSO

258 (Zhang et al., 2014b). Their model estimations indicated that higher DMSO concentrations

259 would lead to enhanced chemical production of MSA to reach 4.9×10^7 molecules cm^{-2} s^{-1},

260 which is similar to the strength of the missing source of MSA.

261 Here, we show that during daytime the reactions of light-excited SO$_2$ and aqueous DMSO or

262 DMSO/PAHs could represent an important source of gaseous MSA in the atmosphere near the

263 water (ocean, lake and river) surface. Figure 2 shows typical time evolution profiles of MSA

264 formed by the reaction of SO$_2$ with PAHs/DMSO under light irradiation (300nm<λ<700nm).

265 The formation profiles of MSM, EMS, MSIA, MSAOH and ESAOH are shown in Figure S2.
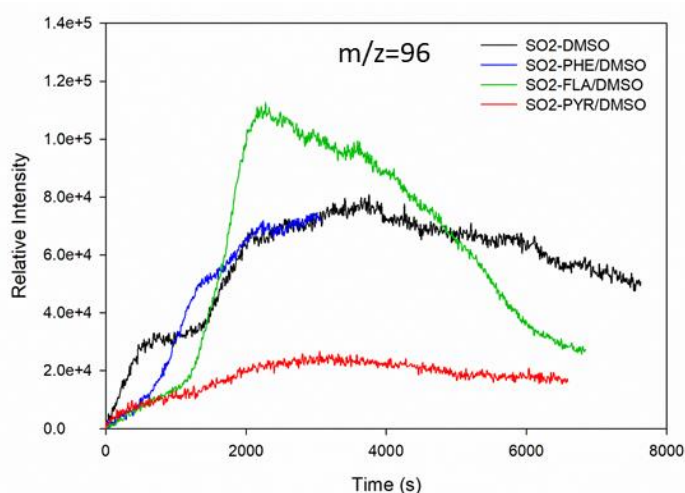
266

267 **Figure 2:** Formation profiles of m/z = 96 (methanesulfonic acid, MSA) upon light-induced
268 heterogeneous reactions of SO$_2$ with DMSO and PAHs/DMSO.

269

270

271 The SO₂ oxidation of FLA/DMSO leads to MSA formation, the signal of which increases

272 during the first 1 hour and then slowly decreases (Figure 2). The intensities of the product

273 compounds (Figure 2 and Figure S2) decrease after one hour most probably due to their reaction

274 with SO₂ and/or their photodegradation. The signal profile of MSA due to reaction of SO₂ with

275 PHE/DMSO is shorter than the others due to a technical problem of the instrument.

276 Intriguingly, the light-induced heterogeneous reaction of SO₂ with DMSO, PYR/DMSO, and

277 PHE/DMSO produces MSA that remains approximately stable over the course of the reaction.

278 These results indicate that the suggested reaction between SO₂ and DMSO or DMSO/PAHs

279 under sunlight irradiation can produce MSA, which can be persistent enough to affect the NPF

280 process in the atmosphere. In section 3.4. we suggest a tentative reaction pathway for the

281 production of MSA and other OSs that is supported by theoretical calculations of Gibbs free

282 energies.

283

284 **3.3. Aqueous OSs Detected by FT-ICR-MS**

285 Numerous unsaturated multifunctional molecules and OSs were identified in the liquid phase

286 during the reaction of SO₂ with either DMSO or PAHs/DMSO by using FT-ICR-MS. The

287 number of detected product compounds in the aqueous phase was significantly higher compared

288 to those detected in the gas phase, due to very high sensitivity of FT-ICR-MS. Figure S3 shows

289 all the formulae detected upon the reaction of SO₂ with PAHs/DMSO under light irradiation.

290 The shared formulae of the compounds detected upon reactions of SO₂ with PYR/DMSO and

291 FLA/DMSO or PHE/DMSO were more abundant than those individually formed by the

292 reaction of SO₂ with FLA/DMSO or PHE/DMSO. The number of detected compounds formed

293 by reaction of SO₂ with PYR/DMSO was dominant among all the products of SO₂ oxidation of

294 PAHs/DMSO, both in the dark and under light irradiation (Figure S3B and S4). Interestingly,

295   the light-induced heterogeneous reaction of SO_2 with PYR/DMSO released a small number of

296   gaseous products, but the highest number of aqueous-phase products among all the studied

297   PAHs/DMSO. In general, more $C_cH_hO_o$ (CHO) than $C_cH_hO_oS_s$ (CHOS) products were formed

298   in the aqueous phase with SO_2 + PAHs/DMSO under irradiation (Figure S5), with the only

299   exception of PHE/DMSO. Even when subtracting the formulae detected upon SO_2 oxidation of

300   DMSO in the dark from those detected in the corresponding light-induced heterogeneous

301   reaction, more compounds were produced under irradiation than in the dark.

302   The analysis of iso-abundance plots of DBE *vs.* carbon numbers for the detected CHO and

303   CHOS formulae is shown in text section S1 and Figures S6-S7. The two-dimensional van

304   Krevelen (VK) plots for all CHOs and CHOSs formed during light-induced SO_2 oxidation of

305   PAHs/DMSO are shown in Figure 3.

306   The CHO and CHOS compounds formed during the reaction of SO_2 with DMSO in the dark

307   and under irradiation are shown in the VK plot depicted in Figure S8. The same classes of

308   compounds, detected upon heterogeneous reactions of SO_2 with PAHs/DMSO under irradiation

309   are illustrated in the VK plots depicted in Figure S9 and Figure S10, respectively. Most of the

310   CHO and CHOS products identified with DMSO had high H/C ratios (1.5-2.1) but O/C ratios

311   lower than 0.4, suggesting the formation of aliphatic compounds (Mekic et al., 2020a). However,

312   the presence of aromatics could be additionally highlighted according to the analysis of a

313   mathematical parameter, the aromaticity equivalent (X_c) (Yassine et al., 2014). About one half

314   of the observed product compounds and especially CHOSs exhibited $X_c \geqslant 2.5$, further

315   indicating the formation of unsaturated compounds during the oxidation of DMSO by SO_2 in

316   the presence of light (Figure S8).

317   The CHO and CHOS products displayed in the VK diagrams of Figure 3 could be all separated

318   into two different clusters. The O/C ratios of CHOs were smaller than 0.7 for SO_2 reaction with

319   PYR/DMSO, and smaller than 0.4 for SO_2 reactions with FLA/DMSO and PHE/DMSO.

320   Nonetheless, a cluster with relatively few observed products was located in the upper part of

321   the VK diagrams with high H/C ratios (1.2-2.0), suggesting the formation of saturated aliphatic

322   CHO compounds.

323

324
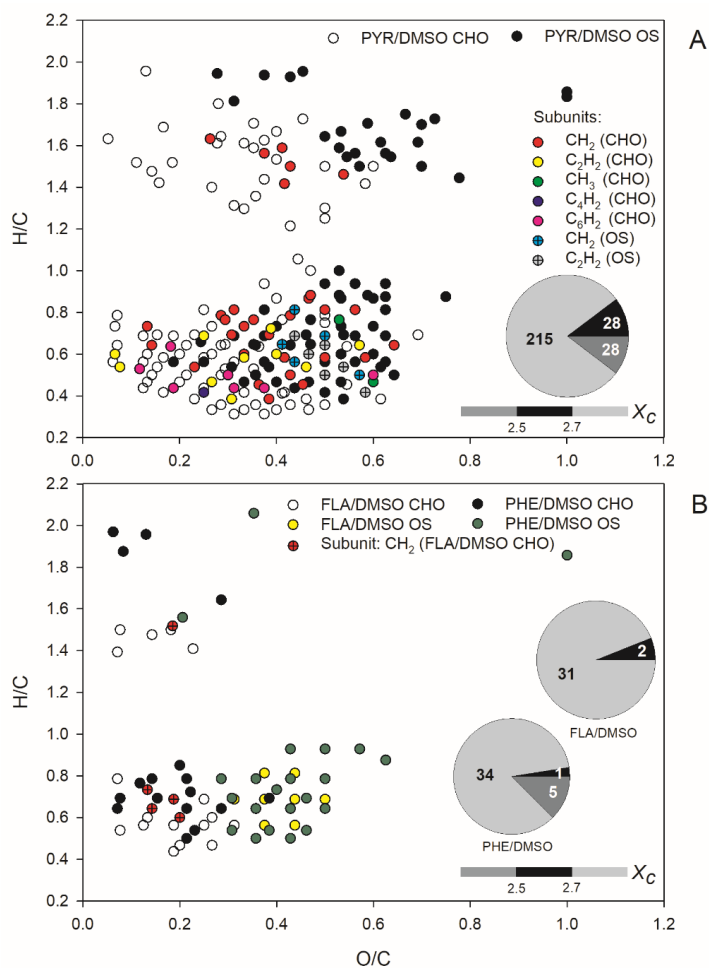
Figure 3: The van Krevelen (VK) graph and aromaticity equivalent (grey with $X_c < 2.5$, black

326   with $2.5 \leqslant X_c < 2.7$, and silver with $X_c \geqslant 2.7$) for the detected CHO and CHOS compounds in

327   ESI⁻ mode, formed upon light-induced heterogeneous reaction of SO_2 with PAHs/DMSO. The

328   X_c value is illustrated by the color bar of each VK diagram, while the pie chart shows the number

329   in different X_c intervals during these reactions.

330

331   The other cluster that includes most of the detected products is located in the lower part of the

332   VK diagrams, exhibiting low H/C ratios (0.4-0.8) and indicating a degree of unsaturation

333   (Mekic et al., 2020a; Lin et al., 2012). Most of the CHO compounds are probably condensed

334   aromatic compounds as suggested by their X_c values higher than 2.5, especially in the case of

335   products observed upon reaction of SO_2 with FLA/DMSO.

336   The observed CHOS products emerging from the reaction of SO_2 with PHE/DMSO, also

337   depicted in Figure 3 could be divided as well into two groups based on their distribution of H/C

338   and O/C ratios. Generally, the formed CHOS products that are located in the upper part of the

339   VK diagrams (Figure 3) have broad range of O/C ratios spanning from 0.2 to 0.8, H/C ratios in

340   a range of 1.4-2.0, and low DBE (1-4). This observation implies the formation of long-chain

341   aliphatic-like CHOSs during the light-assisted oxidation of PHE/DMSO by SO_2. In addition, a

342   big fraction of compounds detected during the reaction of SO_2 with PHE/DMSO exhibits $X_c <$

343   2.5, and is thus consistent with the formation of long-chain aliphatic-like CHOSs (Wang et al.,

344   2021). The CHOS products located in the lower part of the VK diagrams have H/C ratios of

345   0.4-1.0, which are similar to those of the observed CHO products. However, the CHOS

346   compounds exhibit higher O/C ratios that range between 0.2 and 0.8 for the reaction of SO_2

347   with PYR/DMSO, and 0.2-0.6 for the reaction of SO_2 with FLA/DMSO and PHE/DMSO. A

348   possible reason is the occurrence of sulfates with $R\text{-}OSO_3^-$ groups, sulfonates with $R\text{-}SO_3^-$

349   groups and sulfones with $R\text{-}SO_2\text{-}R'$ groups (Bruggemann et al., 2020). These CHOS products

350   partly overlap with the oxidized aromatic hydrocarbons (Kourtchev et al., 2014). Moreover, the

351   majority of the CHOS products exhibit a condensed aromatic structure as indicated by their X_c

352   values higher than 2.7.

353   Based on the VK plots, here we used the different spacing patterns for Kendrick mass defect

354   (KMD) analysis (Lin et al., 2012). The subunits including CH_2, C_2H_2, CH_3, C_4H_2, C_6H_2 for the

355   same CHO homologous series, and CH_2, C_2H_2 for CHOS homologues were identified during

356 the light-induced SO_2 oxidation of PAHs/DMSO. More subunits were found for CHOS

357 homologues during the SO_2 oxidation of PAHs/DMSO under all experimental conditions

358 (Figure S11). Literature suggests that subunits of CH_2 and C_2H_2 were the most repeating mass

359 building increments for either CHO or CHOS oxidized aromatic compounds (Lin et al., 2012).

360 These identified subunits were responsible for the increase in the molecular mass of the detected

361 compounds (Altieri et al., 2006), presumably leading to straight-chain alkanes and olefins.

362 **3.4. Tentative Reaction Mechanisms and the Production of OSs**

363 The proposed general pathway suggested in the literature is the direct addition of SO_2 to a

364 double bond or the separate addition of SO_2 to the cleavage of a double bond. This may also

365 apply to PAHs/DMSO, because of the chromophoric nature of the SO_2 adduct with C=C bonds

366 (Passananti et al., 2016). Herein, we show that this reaction pathway of SO_2 may indeed proceed

367 on PAHs and is supported by theoretical calculations of the reaction Gibbs energies, based on

368 the information obtained from the detected tentative products.

369 The reaction pathway suggests that photoexcitation of PAHs and SO_2 proceeds through the

370 $\pi \rightarrow \pi^*$ electronic transition, followed by intersystem crossing to produce the corresponding

371 excited triplet states (^{3}PAHs* and $^3SO_2$*) (Mekic et al., 2020a), which most likely play an

372 important role during the oxidation of PAHs/DMSO. Previous work concluded that the

373 photochemical reaction of ^{3}PAHs* with DMSO in water would lead to the formation of singlet

374 oxygen ($^1O_2$) *via* energy transfer reaction with ground triplet-state oxygen ($^3O_2$) (Wilkinson et

375 al., 1995), the formation of hydroxyl radical upon water oxidation by other triplets states

376 (Brigante et al., 2010), and the formation of more radicals through electron transfer. Many

377 triplet states work in the presence of oxygen as O_2 quenches most, but not all of them. The

378 excited triplet state of SO_2 ($^3SO_2$*) formed upon light irradiation reacts with water molecules

379 yielding OH radicals as follows (Martins-Costa et al., 2018; Kroll et al., 2018):

380 $^3SO_2^* + H_2O \rightarrow OH + HOSO$ R-1

381 The OH radical attack on PAHs/DMSO yields carbon-centered radicals or alkyl radical which

382 further react with O_2 yielding peroxyl (RO_2) and hydroxyperoxyl radicals (HO_2) (Von Sonntag

383 et al., 1997).

384 Although RO_2 could directly transform into organic sulfates by SO_2, it has been shown that SO_2

385 could accelerate heterogeneous OH oxidation rates by 10 to 20 times, originating from the

386 radical chain reactions propagated by alkoxy radicals formed by the reaction of peroxyl radicals

387 with SO_2 (Richards-Henderson et al., 2016). Peroxyl radicals undergoes self-reactions leading

388 to the formation of stable products (ketone or alcohol) or alkoxy radicals.(Richards-Henderson

389 et al., 2016) In the presence of $^3SO_2^*$, the OH production rate increases by several orders of

390 magnitude at the air-water interface, thus resulting the increase of radical chain length by alkoxy

391 radicals (Martins-Costa et al., 2018).

392 In this study, the comprehensive reaction schemes fully explain the detected sulfur-containing

393 unsaturated multifunctional compounds emerging from light-induced SO_2 oxidation of PAHs

394 and DMSO at the air-water interface. The tentative reaction pathways describing the formation

395 of aqueous-phase products including their description are given in the text section S2 and

396 Scheme S1. The suggested reaction mechanism for the formation of gas-phase product

397 compounds is shown in Scheme 1 in the following section.

398 **3.5. Reaction Mechanism of the Gaseous Compounds**

399 A detailed mechanism for the $^3SO_2^*$ oxidation of PAHs/DMSO is presented in Scheme 1, which

400 could be divided into two proposed general pathways including 1) self-oxidation of $^3SO_2^*$ and

401 oxidation of DMSO initiated by $^3SO_2^*$ and $^3PAH^*$, and 2) photodegradation of sulfur-

402 containing PAH compounds that were initially formed from PAHs by $^3SO_2^*$.

403 *Pathway A*: In this pathway, we emphasize the formation and transformation of MSA that plays

404 a key role during the formation of the detected OSs (Scheme 1A).

405 The self-oxidation of $^3SO_2^*$ could yield sulfuric acid (H_2SO_4) (1). Meanwhile, DMSO can be

406 oxidized by oxygen and the OH radical formed by $^3SO_2^*$ and $^3PAH^*$, yielding MSIA (CH_4O_2S)

407 (2) and MSM ($C_2H_6O_2S$) (3). Dehydration of MSIA (2) (Urbanski et al., 1998; Kukui et al.,

408 2003; Allen et al., 1999; Arsene et al., 2002) and sulfuric acid (1) would lead to the production

409 of MSA (CH_4SO_3) (4). More radical species such as the methyl radical (CH_3), would be formed

410 during the OH-addition route in the gas-phase atmospheric oxidation of DMSO, resulting in the

411 formation of SO_2 that would participate in the subsequent oxidation reactions (Falbe-Hansen et

412 al., 2000; González-García et al., 2006; Arsene et al., 2002; Urbanski et al., 1998).

413 Further transformation would occur upon oxidation of MSA (4) or self-oxidation of $^3SO_2^*$ to

414 yield MSAOH (CH_4O_4S) (5) via OH_2 radical. The OH and CH_2OH radicals could oxidize MSA

415 (4) into ESAOH ($C_2H_6O_4S$) (6) and $C_2H_6O_3S$ (7).

416 *Pathway B*: Although linear OS products would also be generated upon addition of $^3SO_2^*$ to

417 double bonds, formed after ring-opening of the PAH molecules, we stress that the occurrence

418 of gaseous OSs mostly emerges from the photodegradation of aromatic OS products. Under our

419 experimental conditions, $^3SO_2^*$ oxidation of PAHs would prevail over PAH photodegradation

420 and would lead to sulfur-containing PAHs. Here we only present the general degradation

421 process and one proposed pathway for the given species. The details of intermediate products

422 were not shown in this scheme.

423 For example, $C_9H_8O_4S$ (9), $C_{10}H_6O_3S$ (10), and $C_{10}H_6O_4S$ (11) (Scheme 1B) appear as the

424 photodegradation products of $C_{16}H_{10}O_3S$ or $C_{16}H_{12}O_3S$, $C_{14}H_{10}O_3S$ and $C_{14}H_{10}O_4S$ (Scheme

425 S1). These compounds were further transformed upon oxygen attack, then followed by cleavage

426 of the phenyl ring through a highly exoergic process. Cleavage of the five-member ring

427 would yield $C_{10}H_8O_3S$ (12) and $C_{10}H_8O_4S$ (13), followed by the yield of phenyl hydrogen

428 sulfate ($C_6H_6O_4S$) (14) via phenyl-ring cleavage. Meanwhile, phenyl-ring cleavage of

429 condensed aromatics would also yield $C_5H_6O_4S$ (15) and 1,3,2-dioxathiole 2,2-dioxide

430   ($C_2H_4O_4S$) (16). Subsequently, the attack of oxygen or radicals initiates the exoergonic opening

431   of a five-member ring or a phenyl ring, resulting in linear OSs under a rapid oxidative scission.

Scheme 1: Detailed reaction mechanism describing the formation of OSs gas-phase products initiated by ³PAHs* and ³SO₂*. Numbers in brackets, written below each molecule, present compound designations to follow better the discussion in the main text.

3.6. Comparison with OSs Identified Within Atmospheric Aerosols

400 Table S6 shows the intercomparison of the OSs detected here, mainly formed upon light-

401 induced reactions of SO_2 with PAHs/DMSO, with OSs identified during various field

402 campaigns. It should be stressed that the agreement between the chemical formulae of the OSs

403 detected in this study and those from field campaigns does not necessarily imply the same

404 molecular structure, because multiple structural isomers are plausible for each formula (Mekic

405 et al., 2020a; Nizkorodov et al., 2011). A total of 81 tentative OSs from this study overlapped

406 with those identified in ambient aerosol samples, wherein 33 OS formulae were detected in the

407 aqueous phase. Only 4 liquid-phase OS formulae were detected following the reactions of SO_2

408 with PAH/DMSO in the dark. The blue-shaded OSs are generated exclusively by the reaction

409 of SO_2 with DMSO. The group of compounds with yellow-shaded area are produced by the

410 reaction of SO_2 with PAHs/DMSO. Finally, the green-shaded area summarizes the OSs

411 detected with both SO_2 + DMSO and SO_2 + PAHs/DMSO. Most of the liquid-phase OS

412 formulae (chemical formulae in bold) were formed individually upon SO_2 oxidation of

413 PYR/DMSO and DMSO. The product compounds individually formed by the reaction of SO_2

414 with PHE/DMSO and the shared formulae generated by the reaction of SO_2 with DMSO and

415 PAHs/DMSO make the biggest contribution to the gas-phase OSs. These observations highlight

416 the importance of the SO_2 oxidation reactions of DMSO and/or PAHs/DMSO at the freshwater

417 and sea surface, or in the liquid films of the aerosol particles, which would represent an

418 important source of OSs.

419 Tentatively identified VOC precursors are also highlighted in Table S6. The tentative

420 precursors of more than half of the identified OSs in the atmosphere still remain unexplained

421 and unknown. Most of the identified overlapped OSs are probably long alkyl chain OSs, thus

422 their tentative precursors were designated as alkyl-containing OSs from anthropogenic sources

423 (Tao et al., 2014). There are three overlapped compounds which were assumed as aromatic OSs,

425   thus their precursors were considered as 2-MeNAP and methylbenzyl sulfate (Staudt et al., 2014;

426   Riva et al., 2015).

427   Figure 4 shows the iso-abundance plot of DBE *vs.* carbon numbers according to the

428   corresponding X_c of liquid-phase OS formulae, intuitively indicating that most of the identified

429   OS formulae with low DBE are presumably long-chain aliphatic-like compounds. Moreover,

430   there were seven detected OSs with aromatic structure that were consistent with those identified

431   in aerosol samples from field studies. Among those aromatic OSs, only $C_8H_8O_5S$ has its

432   tentatively identified VOC precursor, 2-MeNAP (Riva et al., 2015). It has been shown that

433   aromatic OSs are produced from the interaction of aromatics with sulfur-containing species.

434   For example, the gas-phase photo-oxidation of PAHs in the presence of sulfate aerosol, and the

435   aqueous-phase reactions of several monocyclic aromatics with sulfite in the presence of Fe^{3+}

436   mediated by sulfoxy radical anions can generate aromatic OSs (Riva et al., 2015; Huang et al.,

437   2020). The reaction of SOA particles formed from photo-oxidation of biodiesel and diesel fuel

438   with SO_2 was demonstrated to yield a large number of aromatic OS species(Blair et al., 2017).
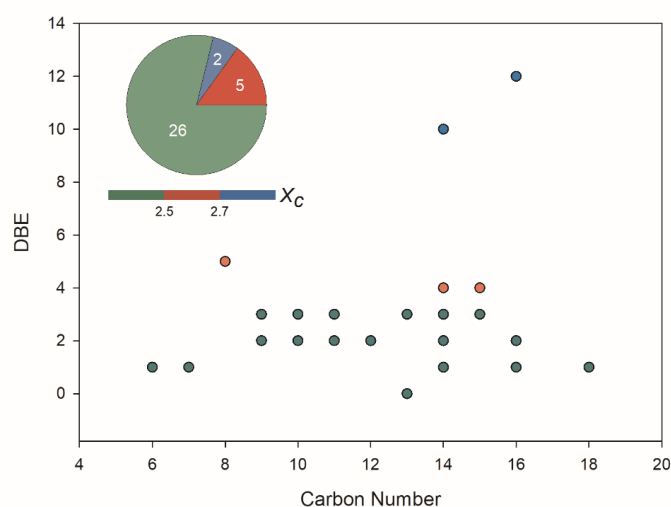
439

440   **Figure 4**: Iso-abundance plot of DBE *vs* carbon numbers according to the corresponding

441   aromaticity equivalent (green with $X_c < 2.5$, red with $2.5 \leqslant X_c < 2.7$, and blue with $X_c \geqslant 2.7$)

442   for the detected organic sulfur species in the liquid phase, which had also been identified in

443   ambient aerosol samples.

444   In our previous study we have identified the OSs formed in the absence of SO_2 as a precursor,

445   during the photodegradation of DMSO initiated by the excited triplet state of fluorene in both

446   liquid and gas phase (Mekic et al., 2020a; Mekic et al., 2020b). It is evident that the inclusion

447   of SO_2 as a precursor in the reaction system enhances the formation of OSs, including those

448   having similar structures as those detected in field studies. It can be considered that the light-

449   induced reaction of SO_2 with DMSO or a mixture of DMSO and PAHs is a previously unknown,

450   additional atmospheric source of OSs (Berresheim et al., 1993; Berresheim and Eisele, 1998;

451   Karl et al., 2007; Hopkins et al., 2008; Gaston et al., 2010; Ning et al., 2020; Dawson et al.,

452   2012).

453   Here we show that light-induced heterogeneous processing of SO_2 with PAHs/DMSO

454   represents an additional source of organic sulphur compounds in the atmosphere and in the

455   freshwater or seawater. In particular, the reaction of SO_2 with DMSO leads to enhanced

456   formation of organic sulphur compounds compared to the photosensitized degradation of

457   DMSO initiated by the excited triplet states of PAHs compounds (Figure S13). This research

458   results point out to the complexity of the chemical processes responsible for the formation of

459   organic sulphur compounds. Considering the abundance of SO_2 in the atmosphere and the

460   omnipresence of water adsorbed PAHs and DMSO compounds, the future modelling studies

461   should consider both pathways, 1) photosensitized degradation of DMSO initiated by the

462   excited triplet states of PAHs (Zhang et al., 2019; Jiang et al., 2021), and 2) heterogeneous

463   chemistry of SO_2 with PAHs/DMSO and DMSO, as alternative formation pathways of organic

464   sulphur compounds in the atmosphere. In this study, many detected aromatic and linear OSs

465   formed during the light-induced SO_2 oxidation of PAHs/DMSO are reported for the first time.

466   An important number of detected compounds overlapped with those of ambient OSs identified

467 during field measurements. We suggest that a plausible mechanism for OSs formation *via* direct

468 addition of SO_2 to the C=C double bond is not only limited to unsaturated acids but is also valid

469 for anthropogenic precursors such as PAHs. A large amount of organosulfates and especially

470 aromatic organosulfates could be formed through this pathway and released into water and

471 ambient atmosphere. These OSs can form surfactant films on aerosol particles in the boundary

472 layer, by which means they influence the surface tension and hygroscopicity of particles

473 (Decesari et al., 2011; Tao et al., 2014). Indeed, the OSs formation pathway in the

474 heterogeneous reaction between SO_2 and PAHs/DMSO is of great significance because OSs

475 generation at the water surface would influence the air-water exchange, and enhanced gaseous

476 OSs would result in the formation of SOA. Moreover, the OS products formation from PAHs

477 initiated by SO_2 is also of importance in urban areas where PAH concentrations are usually

478 high in ambient air (Zhu et al., 2019; Cai et al., 2020). Finally, aromatic OSs occurring in urban

479 aerosols represent a still unrecognized source of toxic products (Riva et al., 2015).

480

Supporting Information

Additional 16 figures, 6 tables and 1 reaction scheme. Short description of MI-SPI-TOF-MS and FT‑ICR‑MS. Analysis of FT‑ICR‑MS aqueous phase products based on DBE vs carbon number iso-abundance plot. Reaction mechanism of the aqueous phase product compounds.

Acknowledgements

This study was financially supported by National Natural Science Foundation of China (N°: 42007200, N°: 41773131, N°: 41977187, and N°: 42177087), Guangdong Foundation for Program of Science and Technology Research (Nº: 2021A1515011555), and China Postdoctoral Science Foundation (Nº: 2019M653105). This study was funded by Institute Director Foundation of GIG (Nº: 2019SZJJ-10), International Cooperation Grant of Chinese Academy of Science (N°: 132744KYSB20190007), State Key Laboratory of Organic Geochemistry, Guangzhou Institute of Geochemistry (SKLOG2020-5, and KTZ_17101). The authors thank Dr. Jiangping Liu, Huifan Deng, Wentao Zhou and Gwendal Loisel for their assistance in the lab analysis. All data in this manuscript are freely available upon request through the corresponding author (gligorovski@gig.ac.cn). This is a contribution of the GIGCAS.

Author Contributions

H.J. and S.G. wrote the paper; S.G. designed the research; H.J. and Y.W. performed the laboratory experiments; H.J. interpreted the MI-SPI-TOF-MS and FT-ICR-MS data and relevant discussion; H.J. Y.H and S.L speculated reaction pathways; Y.H. carried out the Gibbs energies theoretical calculation of the reaction initiated by ^{3}PAH* and ^{3}SO$_2$*; B.J. contributed to the FT-ICR-MS data analysis. X.L. contributed to the MI-SPI-TOF-MS data analysis, L.Y. and T.L. contributed to the relevant discussion of reaction mechanisms; L.C., and D.V.

506   contributed to the discussion of the results and implications. All the authors contributed to

507   revise the manuscript and approved the final version.

508

509   **Author information**

510   Corresponding Author

511   * Phone: +86 2085291497; Email: gligorovski@gig.ac.cn

512

513   **Notes**

514   The authors declare no competing financial interest.

515

516

517 **References**

518 Allen, H. C., Gragson, D., and Richmond, G.: Molecular structure and adsorption of dimethyl sulfoxide
519 at the surface of aqueous solutions, J. Phys. Chem. B, 103, 660-666, 1999.
520 Altieri, K. E., Carlton, A. G., Lim, H.-J., Turpin, B. J., and Seitzinger, S. P.: Evidence for oligomer formation
521 in clouds: Reactions of isoprene oxidation products, Environ. Sci. Technol., 40, 4956-4960,
522 10.1021/es052170n, 2006.
523 Andreae, M. O. J. L.: Dimethylsulfoxide in marine and freshwaters, Limnol. Oceanogr., 25, 1054-1063,
524 1980.
525 Arsene, C., Barnes, I., Becker, K. H., Schneider, W. F., Wallington, T. T., Mihalopoulos, N., and Patroescu-
526 Klotz, I. V. J. E. s.: Formation of methane sulfinic acid in the gas-phase OH-radical initiated oxidation of
527 dimethyl sulfoxide, Environ. Sci. Technol., 36, 5155-5163, 2002.
528 Asher, E., Dacey, J. W., Ianson, D., Peña, A., and Tortell, P. D.: Concentrations and cycling of DMS, DMSP,
529 and DMSO in coastal and offshore waters of the Subarctic Pacific during summer, 2010‐2011, J.
530 Geophys. Res. Oceans, 122, 3269-3286, 2017.
531 Barnes, I., Hjorth, J., and Mihalopoulos, N.: Dimethyl sulfide and dimethyl sulfoxide and their oxidation
532 in the atmosphere, Chem. Rev., 106, 940-975, 10.1021/cr020529+, 2006.
533 Benson, N. U., Essien, J. P., Asuquo, F. E., and Eritobor, A. L.: Occurrence and distribution of polycyclic
534 aromatic hydrocarbons in surface microlayer and subsurface seawater of Lagos Lagoon, Nigeria,
535 Environ. Monit. Assess., 186, 5519-5529, 2014.
536 Berresheim, H. and Eisele, F.: Sulfur chemistry in the Antarctic Troposphere Experiment: An overview
537 of project SCATE, J. Geophys. Res-Atmos, 103, 1619-1627, 1998.
538 Berresheim, H., Eisele, F., Tanner, D., McInnes, L., Ramsey‐Bell, D., and Covert, D.: Atmospheric sulfur
539 chemistry and cloud condensation nuclei (CCN) concentrations over the northeastern Pacific coast, J.
540 Geophys. Res-Atmos, 98, 12701-12711, 1993.
541 Berresheim, H., Elste, T., Tremmel, H. G., Allen, A. G., Hansson, H. C., Rosman, K., Dal Maso, M., Makela,
542 J. M., Kulmala, M., and O'Dowd, C. D.: Gas-aerosol relationships of H2SO4, MSA, and OH: Observations
543 in the coastal marine boundary layer at Mace Head, Ireland, J. Geophys. Res-Atmos, 107,
544 10.1029/2000jd000229, 2002.
545 Binning Jr, R. and Curtiss, L.: Compact contracted basis sets for third‐row atoms: Ga‐Kr, J. Comput.
546 Chem., 11, 1206-1216, 1990.
547 Blair, S. L., MacMillan, A. C., Drozd, G. T., Goldstein, A. H., Chu, R. K., Paša-Tolić, L., Shaw, J. B., Tolić, N.,
548 Lin, P., and Laskin, J.: Molecular characterization of organosulfur compounds in biodiesel and diesel
549 fuel secondary organic aerosol, Environ. Sci. Technol., 51, 119-127, 2017.
550 Bork, N., Elm, J., Olenius, T., and Vehkamaki, H.: Methane sulfonic acid-enhanced formation of
551 molecular clusters of sulfuric acid and dimethyl amine, Atmospheric Chem. Phys., 14, 12023-12030,
552 10.5194/acp-14-12023-2014, 2014.
553 Brigante, M., Charbouillot, T., Vione, D., and Mailhot, G.: Photochemistry of 1-nitronaphthalene: A
554 potential source of singlet oxygen and radical species in atmospheric waters, J. Phys. Chem. A, 114,
555 2830-2836, 2010.
556 Brimblecombe, P. and Shooter, D.: Photo-oxidation of dimethylsulphide in aqueous solution, Mar.
557 Chem., 19, 343-353, 1986.
558 Bruggemann, M., Xu, R., Tilgner, A., Kwong, K. C., Mutzel, A., Poon, H. Y., Otto, T., Schaefer, T., Poulain,
559 L., Chan, M. N., and Herrmann, H.: Organosulfates in Ambient Aerosol: State of Knowledge and Future
560 Research Directions on Formation, Abundance, Fate, and Importance, Environ. Sci. Technol., 54, 3767-
561 3782, 10.1021/acs.est.9b06751, 2020.
562 Cai, D., Wang, X., Chen, J., and Li, X.: Molecular Characterization of Organosulfates in Highly Polluted
563 Atmosphere Using Ultra-High-Resolution Mass Spectrometry, J. Geophys. Res-Atmos, 125,
564 10.1029/2019jd032253, 2020.

565 Chen, H., Varner, M. E., Gerber, R. B., and Finlayson-Pitts, B. J.: Reactions of Methanesulfonic Acid with
566 Amines and Ammonia as a Source of New Particles in Air, J. Phys. Chem. B, 120, 1526-1536,
567 10.1021/acs.jpcb.5b07433, 2016.
568 Chen, J., Ehrenhauser, F. S., Valsaraj, K. T., and Wornat, M. J.: Uptake and UV-photooxidation of gas-
569 phase PAHs on the surface of atmospheric water films. 1. Naphthalene, J. Phys. Chem. A, 110, 9161-
570 9168, 2006.
571 Chen, Q., Sherwen, T., Evans, M., and Alexander, B.: DMS oxidation and sulfur aerosol formation in the
572 marine troposphere: a focus on reactive halogen and multiphase chemistry, Atmospheric Chem. Phys.,
573 18, 13617-13637, 10.5194/acp-18-13617-2018, 2018.
574 Cincinelli, A., Stortini, A. M., Perugini, M., Checchini, L., and Lepri, L.: Organic pollutants in sea-surface
575 microlayer and aerosol in the coastal environment of Leghorn - (Tyrrhenian Sea), Mar. Chem., 76, 77-
576 98, 10.1016/s0304-4203(01)00049-4, 2001.
577 Dall'Osto, M., Ceburnis, D., Monahan, C., Worsnop, D. R., Bialek, J., Kulmala, M., Kurten, T., Ehn, M.,
578 Wenger, J., Sodeau, J., Healy, R., and O'Dowd, C.: Nitrogenated and aliphatic organic vapors as possible
579 drivers for marine secondary organic aerosol growth, J. Geophys. Res-Atmos, 117,
580 10.1029/2012jd017522, 2012.
581 Davidovits, P., Kolb, C. E., Williams, L. R., Jayne, J. T., and Worsnop, D. R.: Mass accommodation and
582 chemical reactions at gas– liquid interfaces, Chem. Rev., 106, 1323-1354, 2006.
583 Dawson, M. L., Varner, M. E., Perraud, V., Ezell, M. J., Gerber, R. B., and Finlayson-Pitts, B. J.: Simplified
584 mechanism for new particle formation from methanesulfonic acid, amines, and water via experiments
585 and ab initio calculations, Proc. Natl. Acad. Sci. U.S.A., 109, 18719-18724, 2012.
586 Decesari, S., Finessi, E., Rinaldi, M., Paglione, M., Fuzzi, S., Stephanou, E., Tziaras, T., Spyros, A.,
587 Ceburnis, D., and O'Dowd, C.: Primary and secondary marine organic aerosols over the North Atlantic
588 Ocean during the MAP experiment, J. Geophys. Res-Atmos, 116, 2011.
589 Deng, H., Liu, J., Wang, Y., Song, W., Wang, X., Li, X., Vione, D., and Gligorovski, S.: Effect of Inorganic
590 Salts on N-Containing Organic Compounds Formed by Heterogeneous Reaction of NO2 with Oleic Acid,
591 Environ. Sci. Technol., 55, 7831-7840, 10.1021/acs.est.1c01043, 2021.
592 Donaldson, D., Kahan, T., Kwamena, N., Handley, S., and Barbier, C.: Atmospheric chemistry of urban
593 surface films, in: Atmospheric Aerosols Characterization, Chemistry, Modeling, and Climate, ACS
594 Publications, 79-89, 2009.
595 Falbe-Hansen, H., Sørensen, S., Jensen, N., Pedersen, T., and Hjorth, J.: Atmospheric gas-phase
596 reactions of dimethylsulphoxide and dimethylsulphone with OH and NO3 radicals, Cl atoms and ozone,
597 Atmos. Environ., 34, 1543-1551, 2000.
598 Frisch, M., Trucks, G., Schlegel, H., Scuseria, G., Robb, M., Cheeseman, J., Scalmani, G., Barone, V.,
599 Petersson, G., and Nakatsuji, H.: Gaussian 16, revision C. 01, 2016.
600 Gaston, C. J., Pratt, K. A., Qin, X., and Prather, K. A.: Real-time detection and mixing state of
601 methanesulfonate in single particles at an inland urban location during a phytoplankton bloom,
602 Environ. Sci. Technol., 44, 1566-1572, 2010.
603 González-García, N., González-Lafont, À., and Lluch, J. M.: Variational transition-state theory study of
604 the dimethyl sulfoxide (DMSO) and OH reaction, J. Phys. Chem.A, 110, 798-808, 2006.
605 González-Gaya, B., Fernández-Pinos, M.-C., Morales, L., Méjanelle, L., Abad, E., Piña, B., Duarte, C. M.,
606 Jiménez, B., and Dachs, J.: High atmosphere–ocean exchange of semivolatile aromatic hydrocarbons,
607 Nat. Geosci, 9, 438-442, 10.1038/ngeo2714, 2016.
608 González-Gaya, B., Martínez-Varela, A., Vila-Costa, M., Casal, P., Cerro-Gálvez, E., Berrojalbiz, N.,
609 Lundin, D., Vidal, M., Mompeán, C., and Bode, A.: Biodegradation as an important sink of aromatic
610 hydrocarbons in the oceans, Nat. Geosci, 12, 119-125, 2019.
611 Grossman, J. N., Stern, A. P., Kirich, M. L., and Kahan, T. F.: Anthracene and pyrene photolysis kinetics
612 in aqueous, organic, and mixed aqueous-organic phases, Atmos. Environ., 128, 158-164, 2016.
613 Guitart, C., Garcia-Flor, N., Bayona, J. M., and Albaiges, J.: Occurrence and fate of polycyclic aromatic
614 hydrocarbons in the coastal surface microlayer, Mar. Pollut. Bull., 54, 186-194,
615 10.1016/j.marpolbul.2006.10.008, 2007.

616 Hardy, J. T., Crecelius, E. A., Antrim, L. D., Kiesser, S. L., Broadhurst, V. L., Boehm, P. D., Steinhauer, W.
617 G., and Coogan, T. H.: Aquatic surface microlayer contamination in chesapeake bay, Mar. Chem., 28,
618 333-351, 1990.
619 Harvey, G. R. and Lang, R. F.: Dimethylsulfoxide and dimethylsulfone in the marine atmosphere,
620 Geophys. Res. Lett., 13, 49-51, 1986.
621 Hatton, A., Malin, G., Turner, S., and Liss, P.: DMSO, A Significant Compound in the Biogeochemical
622 Cycle of DMS., in: Biological and Environmental Chemistry of DMSP and Related Sulfonium Compounds,
623 Springer, 405-412, 1996.
624 Hoffmann, E. H., Tilgner, A., Schrodner, R., Brauer, P., Wolke, R., and Herrmann, H.: An advanced
625 modeling study on the impacts and atmospheric implications of multiphase dimethyl sulfide chemistry,
626 Proc Natl Acad Sci U S A, 113, 11776-11781, 10.1073/pnas.1606320113, 2016.
627 Hopkins, R. J., Desyaterik, Y., Tivanski, A. V., Zaveri, R. A., Berkowitz, C. M., Tyliszczak, T., Gilles, M. K.,
628 and Laskin, A.: Chemical speciation of sulfur in marine cloud droplets and particles: Analysis of
629 individual particles from the marine boundary layer over the California current, J. Geophys. Res-Atmos,
630 113, 2008.
631 Huang, L., Liu, T., and Grassian, V. H.: Radical-Initiated Formation of Aromatic Organosulfates and
632 Sulfonates in the Aqueous Phase, Environ. Sci. Technol., 54, 11857-11864, 10.1021/acs.est.0c05644,
633 2020.
634 Jiang, B., Kuang, B. Y., Liang, Y., Zhang, J., Huang, X. H. H., Xu, C., Yu, J. Z., and Shi, Q.: Molecular
635 composition of urban organic aerosols on clear and hazy days in Beijing: a comparative study using FT-
636 ICR MS, Environ. Chem., 13, 888-901, 10.1071/en15230, 2016.
637 Jiang, H., Carena, L., He, Y., Wang, Y., Zhou, W., Yang, L., Luan, T., Li, X., Brigante, M., Vione, D., and
638 Gligorovski, S.: Photosensitized degradation of DMSO initiated by PAHs at the air-water interface, as
639 an alternative source of organic sulfur compounds to the atmosphere, J. Geophys. Res-Atmos, 126,
640 10.1029/2021JD035346, 2021.
641 Kamens, R. M., Zhang, H., Chen, E. H., Zhou, Y., Parikh, H. M., Wilson, R. L., Galloway, K. E., and Rosen,
642 E. P.: Secondary organic aerosol formation from toluene in an atmospheric hydrocarbon mixture:
643 Water and particle seed effects, Atmos. Environ., 45, 2324-2334, 10.1016/j.atmosenv.2010.11.007,
644 2011.
645 Karl, M., Gross, A., Leck, C., and Pirjola, L.: Intercomparison of dimethylsulfide oxidation mechanisms
646 for the marine boundary layer: Gaseous and particulate sulfur constituents, J. Geophys. Res-Atmos,
647 112, 10.1029/2006jd007914, 2007.
648 Kourtchev, I., O'Connor, I. P., Giorio, C., Fuller, S. J., Kristensen, K., Maenhaut, W., Wenger, J. C., Sodeau,
649 J. R., Glasius, M., and Kalberer, M.: Effects of anthropogenic emissions on the molecular composition
650 of urban organic aerosols: An ultrahigh resolution mass spectrometry study, Atmos. Environ., 89, 525-
651 532, 10.1016/j.atmosenv.2014.02.051, 2014.
652 Kroll, J. A., Frandsen, B. N., Kjaergaard, H. G., and Vaida, V.: Atmospheric hydroxyl radical source:
653 Reaction of triplet SO2 and water, J. Phys. Chem.A, 122, 4465-4469, 2018.
654 Kukui, A., Borissenko, D., Laverdet, G., and Le Bras, G.: Gas-phase reactions of OH radicals with
655 dimethyl sulfoxide and methane sulfinic acid using turbulent flow reactor and chemical ionization mass
656 spectrometry, J. Phys. Chem.A, 107, 5732-5742, 2003.
657 Kundu, S., Quraishi, T. A., Yu, G., Suarez, C., Keutsch, F. N., and Stone, E. A.: Evidence and quantitation
658 of aromatic organosulfates in ambient aerosols in Lahore, Pakistan, Atmospheric Chem. Phys., 13,
659 4865-4875, 10.5194/acp-13-4865-2013, 2013.
660 Lammel, G.: Polycyclic aromatic compounds in the atmosphere–a review identifying research needs,
661 Polycyclic Aromat. Compd., 35, 316-329, 2015.
662 Lee, P. and De Mora, S.: DMSP, DMS and DMSO concentrations and temporal trends in marine surface
663 waters at Leigh, New Zealand, in: Biological and Environmental Chemistry of DMSP and Related
664 Sulfonium Compounds, Springer, 391-404, 1996.
665 Lee, P. A., de Mora, S. J., and Levasseur, M.: A review of dimethylsulfoxide in aquatic environments,
666 Atmosphere-Ocean, 37, 439-456, 10.1080/07055900.1999.9649635, 1999.

667   Legrand, M., Sciare, J., Jourdain, B., and Genthon, C.: Subdaily variations of atmospheric
668   dimethylsulfide, dimethylsulfoxide, methanesulfonate, and non‐sea‐salt sulfate aerosols in the
669   atmospheric boundary layer at Dumont d'Urville (coastal Antarctica) during summer, J. Geophys. Res-
670   Atmos, 106, 14409-14422, 2001.
671   Li, G., Bei, N., Cao, J., Huang, R., Wu, J., Feng, T., Wang, Y., Liu, S., Zhang, Q., Tie, X., and Molina, L. T.:
672   A possible pathway for rapid growth of sulfate during haze days in China, Atmospheric Chem. Phys.,
673   17, 3301-3316, 10.5194/acp-17-3301-2017, 2017a.
674   Li, J., Li, F., and Liu, Q.: PAHs behavior in surface water and groundwater of the Yellow River estuary:
675   evidence from isotopes and hydrochemistry, Chemosphere, 178, 143-153, 2017b.
676   Librando, V., Tringali, G., Hjorth, J., and Coluccia, S.: OH-initiated oxidation of DMS/DMSO: reaction
677   products at high NOx levels, Environ. Pollut., 127, 403-410, 2004.
678   Librando, V., Bracchitta, G., de Guidi, G., Minniti, Z., Perrini, G., and Catalfo, A.: Photodegradation of
679   anthracene and benzo [a] anthracene in polar and apolar media: new pathways of photodegradation,
680   Polycyclic Aromat. Compd., 34, 263-279, 2014.
681   Lin, P., Rincon, A. G., Kalberer, M., and Yu, J. Z.: Elemental composition of HULIS in the Pearl River Delta
682   Region, China: results inferred from positive and negative electrospray high resolution mass
683   spectrometric data, Environ. Sci. Technol., 46, 7454-7462, 10.1021/es300285d, 2012.
684   Lohmann, R., Gioia, R., Jones, K. C., Nizzetto, L., Temme, C., Xie, Z., Schulz-Bull, D., Hand, I., Morgan, E.,
685   and Jantunen, L. J. E. s.: Organochlorine pesticides and PAHs in the surface water and atmosphere of
686   the North Atlantic and Arctic Ocean, Environ. Sci. Technol., 43, 5633-5639, 2009.
687   Ma, Y., Xu, X., Song, W., Geng, F., and Wang, L.: Seasonal and diurnal variations of particulate
688   organosulfates in urban Shanghai, China, Atmos. Environ., 85, 152-160,
689   10.1016/j.atmosenv.2013.12.017, 2014.
690   Ma, Y., Xie, Z., Yang, H., Möller, A., Halsall, C., Cai, M., Sturm, R., and Ebinghaus, R.: Deposition of
691   polycyclic aromatic hydrocarbons in the North Pacific and the Arctic, J. Geophys. Res-Atmos, 118, 5822-
692   5829, 2013.
693   Martins-Costa, M. T., Anglada, J. M., Francisco, J. S., and Ruiz-López, M. F.: Photochemistry of SO2 at
694   the air–water interface: a source of OH and HOSO radicals, J. Am. Chem. Soc., 140, 12341-12344, 2018.
695   McLean, A. and Chandler, G.: Contracted Gaussian basis sets for molecular calculations. I. Second row
696   atoms, Z= 11–18, J. Chem. Phys., 72, 5639-5648, 1980.
697   Mekic, M., Zeng, J., Jiang, B., Li, X., Lazarou, Y. G., Brigante, M., Herrmann, H., and Gligorovski, S.:
698   Formation of Toxic Unsaturated Multifunctional and Organosulfur Compounds From the
699   Photosensitized Processing of Fluorene and DMSO at the Air‐Water Interface, J. Geophys. Res-Atmos,
700   125, 10.1029/2019jd031839, 2020a.
701   Mekic, M., Zeng, J., Zhou, W., Loisel, G., Jin, B., Li, X., Vione, D., and Gligorovski, S.: Ionic Strength Effect
702   on Photochemistry of Fluorene and Dimethylsulfoxide at the Air–Sea Interface: Alternative Formation
703   Pathway of Organic Sulfur Compounds in a Marine Atmosphere ACS Earth Space Chem., 4, 1029-1038,
704   10.1021/acsearthspacechem.0c00059, 2020b.
705   Monge, M. E., George, C., D'Anna, B., Doussin, J.-F., Jammoul, A., Wang, J., Eyglunent, G., Solignac, G.,
706   Daele, V., and Mellouki, A.: Ozone formation from illuminated titanium dioxide surfaces, J. Am. Chem.
707   Soc., 132, 8234-8235, 2010.
708   Ning, A., Zhang, H., Zhang, X., Li, Z., Zhang, Y., Xu, Y., and Ge, M.: A molecular-scale study on the role
709   of methanesulfinic acid in marine new particle formation, Atmos. Environ., 227,
710   10.1016/j.atmosenv.2020.117378, 2020.
711   Nizkorodov, S. A., Laskin, J., and Laskin, A.: Molecular chemistry of organic aerosols through the
712   application of high resolution mass spectrometry, PCCP, 13, 3612-3629, 2011.
713   Oppenheimer, C., Francis, P., Burton, M., Maciejewski, A., and Boardman, L.: Remote measurement of
714   volcanic gases by Fourier transform infrared spectroscopy, Appl. Phys. B: Lasers Opt., 67, 1998.
715   Otto, S., Streibel, T., Erdmann, S., Klingbeil, S., Schulz-Bull, D., and Zimmermann, R.: Pyrolysis–gas
716   chromatography–mass spectrometry with electron-ionization or resonance-enhanced-multi-photon-

717 ionization for characterization of polycyclic aromatic hydrocarbons in the Baltic Sea, Mar. Pollut. Bull.,
718 99, 35-42, 2015.
719 Passananti, M., Kong, L., Shang, J., Dupart, Y., Perrier, S., Chen, J., Donaldson, D. J., and George, C.:
720 Organosulfate Formation through the Heterogeneous Reaction of Sulfur Dioxide with Unsaturated
721 Fatty Acids and Long‐Chain Alkenes, Angew. Chem. Int. Ed., 55, 10336-10339, 2016.
722 Pérez-Carrera, E., León, V. M. L., Parra, A. G., and González-Mazo, E.: Simultaneous determination of
723 pesticides, polycyclic aromatic hydrocarbons and polychlorinated biphenyls in seawater and interstitial
724 marine water samples, using stir bar sorptive extraction–thermal desorption–gas chromatography–
725 mass spectrometry, J. Chromatogr. A, 1170, 82-90, 2007.
726 Perraud, V., Horne, J. R., Martinez, A. S., Kalinowski, J., Meinardi, S., Dawson, M. L., Wingen, L. M.,
727 Dabdub, D., Blake, D. R., Gerber, R. B., and Finlayson-Pitts, B. J.: The future of airborne sulfur-containing
728 particles in the absence of fossil fuel sulfur dioxide emissions, Proc Natl Acad Sci U S A, 112, 13514-
729 13519, 10.1073/pnas.1510743112, 2015.
730 Richards-Henderson, N. K., Goldstein, A. H., Wilson, K. R. J. E. s., and technology: Sulfur dioxide
731 accelerates the heterogeneous oxidation rate of organic aerosol by hydroxyl radicals, Environ. Sci.
732 Technol. Lett., 50, 3554-3561, 2016.
733 Richards, S., Rudd, J., and Kelly, C.: Organic volatile sulfur in lakes ranging in sulfate and dissolved salt
734 concentration over five orders of magnitude, Limnol. Oceanogr., 39, 562-572, 1994.
735 Ridgeway, R. G., Thornton, D. C., and Bandy, A. R.: Determination of trace aqueous dimethylsulfoxide
736 concentrations by isotope dilution gas chromatography/mass spectrometry: Application to rain and
737 sea water, J. Atmos. Chem., 14, 53-60, 1992.
738 Riva, M., Da Silva Barbosa, T., Lin, Y.-H., Stone, E. A., Gold, A., and Surratt, J. D.: Chemical
739 characterization of organosulfates in secondary organic aerosol derived from the photooxidation of
740 alkanes, Atmospheric Chem. Phys., 16, 11001-11018, 10.5194/acp-16-11001-2016, 2016.
741 Riva, M., Tomaz, S., Cui, T., Lin, Y. H., Perraudin, E., Gold, A., Stone, E. A., Villenave, E., and Surratt, J.
742 D.: Evidence for an unrecognized secondary anthropogenic source of organosulfates and sulfonates:
743 gas-phase oxidation of polycyclic aromatic hydrocarbons in the presence of sulfate aerosol, Environ.
744 Sci. Technol., 49, 6654-6664, 10.1021/acs.est.5b00836, 2015.
745 Rosati, B., Christiansen, S., de Jonge, R. W., Roldin, P., Jensen, M. M., Wang, K., Moosakutty, S. P.,
746 Thomsen, D., Salomonsen, C., Hyttinen, N., Elm, J., Feilberg, A., Glasius, M., and Bilde, M.: New Particle
747 Formation and Growth from Dimethyl Sulfide Oxidation by Hydroxyl Radicals, ACS Earth Space Chem.,
748 5, 801-811, 10.1021/acsearthspacechem.0c00333, 2021.
749 Schobesberger, S., Junninen, H., Bianchi, F., Lonn, G., Ehn, M., Lehtipalo, K., Dommen, J., Ehrhart, S.,
750 Ortega, I. K., Franchin, A., Nieminen, T., Riccobono, F., Hutterli, M., Duplissy, J., Almeida, J., Amorim,
751 A., Breitenlechner, M., Downard, A. J., Dunne, E. M., Flagan, R. C., Kajos, M., Keskinen, H., Kirkby, J.,
752 Kupc, A., Kurten, A., Kurten, T., Laaksonen, A., Mathot, S., Onnela, A., Praplan, A. P., Rondo, L., Santos,
753 F. D., Schallhart, S., Schnitzhofer, R., Sipila, M., Tome, A., Tsagkogeorgas, G., Vehkamaki, H., Wimmer,
754 D., Baltensperger, U., Carslaw, K. S., Curtius, J., Hansel, A., Petaja, T., Kulmala, M., Donahue, N. M., and
755 Worsnop, D. R.: Molecular understanding of atmospheric particle formation from sulfuric acid and
756 large oxidized organic molecules, Proc Natl Acad Sci U S A, 110, 17223-17228,
757 10.1073/pnas.1306973110, 2013.
758 Seidel, M., Manecki, M., Herlemann, D. P., Deutsch, B., Schulz-Bull, D., Jürgens, K., and Dittmar, T.:
759 Composition and transformation of dissolved organic matter in the Baltic Sea, Front. Earth Sci., 5, 31,
760 2017.
761 Shang, J., Passananti, M., Dupart, Y., Ciuraru, R., Tinel, L., Rossignol, S. p., Perrier, S. b., Zhu, T., and
762 George, C.: SO2 Uptake on oleic acid: A new formation pathway of organosulfur compounds in the
763 atmosphere, Environ. Sci. Technol. Lett., 3, 67-72, 2016.
764 Smith, S. J., Pitcher, H., and Wigley, T. M. L.: Global and regional anthropogenic sulfur dioxide emissions,
765 Global Planet. Change, 29, 99-119, 10.1016/s0921-8181(00)00057-6, 2001.
766 Staudt, S., Kundu, S., Lehmler, H.-J., He, X., Cui, T., Lin, Y.-H., Kristensen, K., Glasius, M., Zhang, X.,
767 Weber, R. J., Surratt, J. D., and Stone, E. A.: Aromatic organosulfates in atmospheric aerosols: Synthesis,

768   characterization, and abundance, Atmos. Environ., 94, 366-373, 10.1016/j.atmosenv.2014.05.049,
769   2014.
770   Stortini, A., Martellini, T., Del Bubba, M., Lepri, L., Capodaglio, G., and Cincinelli, A.: n-Alkanes, PAHs
771   and surfactants in the sea surface microlayer and sea water samples of the Gerlache Inlet sea
772   (Antarctica), Microchem. J., 92, 37-43, 2009.
773   Styler, S., Loiseaux, M.-E., and Donaldson, D.: Substrate effects in the photoenhanced ozonation of
774   pyrene, Atmospheric Chem. Phys., 11, 1243-1253, 2011.
775   Tao, S., Lu, X., Levac, N., Bateman, A. P., Nguyen, T. B., Bones, D. L., Nizkorodov, S. A., Laskin, J., Laskin,
776   A., and Yang, X.: Molecular characterization of organosulfates in organic aerosols from Shanghai and
777   Los Angeles urban areas by nanospray-desorption electrospray ionization high-resolution mass
778   spectrometry, Environ. Sci. Technol., 48, 10993-11001, 2014.
779   Urbanski, S., Stickel, R., and Wine, P.: Mechanistic and kinetic study of the gas-phase reaction of
780   hydroxyl radical with dimethyl sulfoxide, J. Phys. Chem.A, 102, 10522-10529, 1998.
781   Vácha, R., Jungwirth, P., Chen, J., and Valsaraj, K.: Adsorption of polycyclic aromatic hydrocarbons at
782   the air–water interface: Molecular dynamics simulations and experimental atmospheric observations,
783   PCCP, 8, 4461-4467, 2006.
784   Valavanidis, A., Vlachogianni, T., Triantafillaki, S., Dassenakis, M., Androutsos, F., and Scoullos, M.:
785   Polycyclic aromatic hydrocarbons in surface seawater and in indigenous mussels (Mytilus
786   galloprovincialis) from coastal areas of the Saronikos Gulf (Greece), Estuar. Coast. Shelf Sci., 79, 733-
787   739, 2008.
788   von Sonntag, C., Dowideit, P., Fang, X., Mertens, R., Pan, X., Schuchmann, M. N., Schuchmann, H.-P. J.
789   W. S., and Technology: The fate of peroxyl radicals in aqueous solution, Water Sci. Technol., 35, 9-15,
790   1997.
791   Wang, Y., Mekic, M., Li, P., Deng, H., Liu, S., Jiang, B., Jin, B., Vione, D., and Gligorovski, S.: Ionic Strength
792   Effect Triggers Brown Carbon Formation through Heterogeneous Ozone Processing of Ortho-Vanillin,
793   Environ. Sci. Technol., 55, 4553-4564, 10.1021/acs.est.1c00874, 2021.
794   Wang, Y., Zhang, Q., Jiang, J., Zhou, W., Wang, B., He, K., Duan, F., Zhang, Q., Philip, S., and Xie, Y.:
795   Enhanced sulfate formation during China's severe winter haze episode in January 2013 missing from
796   current models, J. Geophys. Res-Atmos, 119, 10.1002/2013jd021426, 2014.
797   Weigend, F.: Accurate Coulomb-fitting basis sets for H to Rn, PCCP, 8, 1057-1065, 2006.
798   Weigend, F. and Ahlrichs, R.: Balanced basis sets of split valence, triple zeta valence and quadruple
799   zeta valence quality for H to Rn: Design and assessment of accuracy, PCCP, 7, 3297-3305, 2005.
800   Wilkinson, F., Helman, W. P., and Ross, A. B.: Rate constants for the decay and reactions of the lowest
801   electronically excited singlet state of molecular oxygen in solution. An expanded and revised
802   compilation, J. Phys. Chem. Ref. Data, 24, 663-677, 1995.
803   Yassine, M. M., Harir, M., Dabek‐Zlotorzynska, E., and Schmitt‐Kopplin, P.: Structural
804   characterization of organic aerosol using Fourier transform ion cyclotron resonance mass
805   spectrometry: aromaticity equivalent approach, Rapid Commun. Mass Spectrom., 28, 2445-2454, 2014.
806   Zhang, L., Kuniyoshi, I., Hirai, M., and Shoda, M.: Oxidation of dimethyl sulfide byPseudomonas
807   acidovorans DMR-11 isolated from peat biofilter, Biotechnol. Lett, 13, 223-228, 1991.
808   Zhang, M., Gao, W., Yan, J., Wu, Y., Marandino, C. A., Park, K., Chen, L., Lin, Q., Tan, G., and Pan, M.:
809   An integrated sampler for shipboard underway measurement of dimethyl sulfide in surface seawater
810   and air, Atmos. Environ., 209, 86-91, 2019.
811   Zhang, S. H., Yang, G. P., Zhang, H. H., and Yang, J.: Spatial variation of biogenic sulfur in the south
812   Yellow Sea and the East China Sea during summer and its contribution to atmospheric sulfate aerosol,
813   Sci. Total Environ., 488-489, 157-167, 10.1016/j.scitotenv.2014.04.074, 2014a.
814   Zhang, Y., Wang, Y., Gray, B. A., Gu, D., Mauldin, L., Cantrell, C., and Bandy, A.: Surface and free
815   tropospheric sources of methanesulfonic acid over the tropical Pacific Ocean, Geophys. Res. Lett., 41,
816   5239-5245, 10.1002/2014gl060934, 2014b.
817   Zhao, H., Jiang, X., and Du, L.: Contribution of methane sulfonic acid to new particle formation in the
818   atmosphere, Chemosphere, 174, 689-699, 10.1016/j.chemosphere.2017.02.040, 2017.

819   Zhao, Y. and Truhlar, D. G.: The M06 suite of density functionals for main group thermochemistry,
820   thermochemical kinetics, noncovalent interactions, excited states, and transition elements: two new
821   functionals and systematic testing of four M06-class functionals and 12 other functionals, Theor. Chem.
822   Acc., 120, 215-241, 2008.
823   Zhou, S., Hwang, B. C. H., Lakey, P. S. J., Zuend, A., Abbatt, J. P. D., and Shiraiwa, M.: Multiphase
824   reactivity of polycyclic aromatic hydrocarbons is driven by phase separation and diffusion limitations,
825   Proc. Natl. Acad. Sci. U. S. A., 116, 11658-11663, 10.1073/pnas.1902517116, 2019.
826   Zhu, M., Jiang, B., Li, S., Yu, Q., Yu, X., Zhang, Y., Bi, X., Yu, J., George, C., and Yu, Z.: Organosulfur
827   Compounds Formed from Heterogeneous Reaction between SO2 and Particulate-Bound Unsaturated
828   Fatty Acids in Ambient Air, Environ. Sci. Technol. Lett., 6, 318-322, 2019.

829